



2

OFFICE OF NAVAL RESEARCH

Grant N00014-90-J-1193

TECHNICAL REPORT No. 85

Theoretical Study of Phase-Shifted Quantum Beats in Time-Resolved Luminescence Spectra from a Biased Asymmetric Double Quantum Well

by

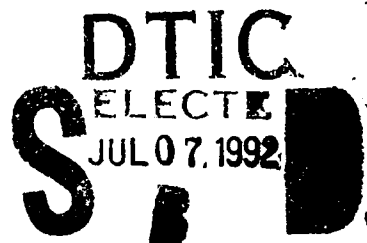
Y. Ohtsuki, Lakshmi N. Pandey and Thomas F. George

Prepared for publication

in

*Chemical Physics Letters*

Departments of Chemistry and Physics  
Washington State University  
Pullman, WA 99164-1046



June 1992

Reproduction in whole or in part is permitted for any purpose of the United States Government.

This document has been approved for public release and sale; its distribution is unlimited.

92-17457



# REPORT DOCUMENTATION PAGE

Form Approved  
OMB No. 0704-0188

Public reporting burden for this collection of information is estimated to average 1 hour per response, including the time for reviewing instructions, searching existing data sources, gathering and maintaining the data needed, and completing and reviewing the collection of information. Send comments regarding this burden estimate or any other aspect of this collection of information, including suggestions for reducing this burden, to Washington Headquarters Services, Directorate for Information Operations and Reports, 1215 Jefferson Davis Highway, Suite 1204, Arlington, VA 22202-4302, and to the Office of Management and Budget, Paperwork Reduction Project (0704-0188), Washington, DC 20503.

1. AGENCY USE ONLY (Leave blank)		2. REPORT DATE June 1992	3. REPORT TYPE AND DATES COVERED Interim	
4. TITLE AND SUBTITLE Theoretical Study of Phase-Shifted Quantum Beats in Time-Resolved Luminescence Spectra from a Biased Asymmetric Double Quantum Well			5. FUNDING NUMBERS Grant N00014-90-J-1193	
6. AUTHOR(S) Y. Ohtsuki, Lakshmi N. Pandey and <u>Thomas F. George</u>				
7. PERFORMING ORGANIZATION NAME(S) AND ADDRESS(ES) Departments of Chemistry and Physics Washington State University			8. PERFORMING ORGANIZATION REPORT NUMBER  WSU/92/85	
9. SPONSORING/MONITORING AGENCY NAME(S) AND ADDRESS(ES) Office of Naval Research 800 N. Quincy Street Arlington, Virginia 22217			10. SPONSORING/MONITORING AGENCY REPORT NUMBER	
11. SUPPLEMENTARY NOTES Prepared for publication in <u>Chemical Physics Letters</u>				
12a. DISTRIBUTION/AVAILABILITY STATEMENT  Approved for public release; distribution unlimited			12b. DISTRIBUTION CODE	
13. ABSTRACT (Maximum 200 words)  Analytical expressions have been developed for time-dependent luminescence intensities for a practically feasible asymmetric double quantum well under bias and numerically demonstrated to elucidate the characteristic of $\pi$ phase-shifted quantum beats. It is clear analytically as well as numerically that the magnitude of the tunneling interaction can be quantitatively estimated by the beat modulation depth.				
14. SUBJECT TERMS QUANTUM BEATS PHASE-SHIFTED LUMINESCENCE SPECTRA TIME-RESOLVED DOUBLE QUANTUM WELL BIASED			15. NUMBER OF PAGES 13 16. PRICE CODE NTIS	
17. SECURITY CLASSIFICATION OF REPORT Unclassified	18. SECURITY CLASSIFICATION OF THIS PAGE Unclassified	19. SECURITY CLASSIFICATION OF ABSTRACT Unclassified	20. LIMITATION OF ABSTRACT	

# **Theoretical Study of Phase-Shifted Quantum Beats in Time-Resolved Luminescence Spectra from a Biased Asymmetric Double Quantum Well**

Y. Ohtsuki<sup>†</sup>

Department of Physics and Astronomy  
State University of New York at Buffalo  
Buffalo, New York 14260

and

Department of Chemistry  
Washington State University  
Pullman, Washington 99163-4630

Lakshmi N. Pandey and Thomas F. George

Departments of Chemistry and Physics  
Washington State University  
Pullman, Washington 99164-2814

Analytical expressions have been developed for time-dependent luminescence intensities for a practically feasible asymmetric double quantum well under bias and numerically demonstrated to elucidate the characteristic of  $\pi$  phase-shifted quantum beats. It is clear analytically as well as numerically that the magnitude of the tunneling interaction can be quantitatively estimated by the beat modulation depth.

PACS Nos: 73.20.Dx, 73.50.Pz, 73.40.Kp, 73.40.Gk



and

$$\langle m | \Gamma \rho(t) | n \rangle = \Gamma_{mn} \rho_{mm}(t) , \quad (m \neq n) , \quad (2b)$$

with an equilibrium distribution  $\rho_{mm}^0$ , where

$$\Gamma_{mm} = \gamma_m , \quad (3a)$$

and

$$\Gamma_{mn} = \frac{\gamma_m + \gamma_n}{2} + \gamma_{mn}^{(pd)} , \quad (m \neq n) . \quad (3b)$$

The Hamiltonian in Eq. (1) includes the zeroth-order Hamiltonian of the relevant system, that of the radiation fields, and the system-radiation interaction under the rotating-wave approximation. We also adopt the phase-diffusion model,<sup>8</sup> in which both the incident and scattered lights are characterized by relaxation constants,  $\Gamma_I$  and  $\Gamma_S$ , respectively. By solving the master equation up to fourth order with respect to the system-radiation interaction, we can obtain the stationary as well as the time-dependent luminescence intensities.

In the following, we adopt a similar structure studied in Ref. 2 and dope the extended barrier regions with a suitable dopant to give free-electrons carriers. Figure 1 shows an illustration of the biased asymmetric DQW, consisting of a 190 Å-GaAs WW, a 80Å-Al<sub>0.1</sub>Ga<sub>0.9</sub>As middle barrier and a 145Å-GaAs NW.<sup>9</sup> In the case of an infinitely-thick middle barrier, each quantum wells has two states,  $|N_k\rangle$  and  $|W_k\rangle$  ( $k = 1, 2$ ), in the NW and WW, respectively. The bias applied to DQW with a moderately thick barrier separating two wells makes these four states quasi-stationary with energy widths, and these quasi-states and their widths are calculated numerically according to the procedure shown in Ref. 10. In the present calculation, we employ two values of bias voltage, one called the resonant voltage at which the energies of the two excited states  $|N_2\rangle$  and  $|W_2\rangle$  coincide with each other<sup>11</sup>, and the other one set at 20% more than the resonant voltage. We assume that only the  $|N_1\rangle$  state of the DQW under bias is populated before the irradiation.

Figure 2 shows the luminescence spectra. The photon energy of the incident light is tuned to the average of the energies of the excited states  $|N_2\rangle$  and  $|W_2\rangle$  which may be align for certain bias. Two sharp peaks correspond to Raman peaks. The two lowest luminescence peaks, labelled L1 and L2, originate from the emission from the states  $|N_2\rangle$  and  $|W_2\rangle$  to the ground state of WW  $|W_1\rangle$ , respectively, while the ground state of the NW  $|N_1\rangle$  is the final state of the other two luminescence components, L3 and L4. The amplitudes of the peaks L1 through L4 depend on the population of the upper two states  $|N_2\rangle$  and  $|W_2\rangle$ , which in turn relate to the probabilities of individual states in each of the

wells. These peaks are discussed further in view of the population of the states later. In Fig. 3, we have calculated the luminescence decay curves whose central frequencies are set to those of the luminescence peaks L3 (solid line) and L1 (dashed line), respectively. We can see the phase-shifted quantum beats in these spectra. Since the initially-created quasi-stationary state is localized in the NW, the luminescence decay curves corresponding to the L3 and L4 peaks show in-phase quantum beats, while those to the L1 and L2 peaks have out-of-phase quantum beats. In these calculations, the envelope function of the incident pulse has been assumed to have the form

$$F(t) = \exp(-\gamma_A)[1 - \exp(-\gamma_B t)] , \quad (4)$$

in which the temporal width has been set to be about a 330-fs full-width at half-maximum (FWHM).<sup>12</sup> In actual experiments, such an ultrafast IR pulse may be realized by the application of the pulse-compression technique using optical fibers.<sup>13</sup> On the other hand, one simultaneously has to prepare an ultrafast detection system for observing the ultrafast response from a nonstationary state. This problem could be solved by using a streak camera measurement<sup>14a</sup> or fluorescence upconversion method.<sup>14b</sup>

Here, to see the characteristics of the beat modulation depths, we have also calculated the normalized out-of-phase and in-phase quantum beats, which are shown in Figure 4. The normalized beat modulation is obtained by dividing the off-diagonal part of the intensity by the diagonal part. These results show the deep modulation of the out-of-phase beat, independent of the value of the bias voltage, i.e., the magnitude of the tunneling interaction. As for the normalized beat modulations of the L3 and L4 components, in the resonant case of the bias voltage, they have almost the same modulation depths as those of the out-of-phase beat components (L1 and L2). However, in the off-resonant case, we can see the small modulation, and the two components have different modulation depths.<sup>15</sup>

To quantitatively understand these results, it is convenient to analyze the analytical expression of the time-dependent luminescence intensity which is derived by assuming a  $\delta$ -function pulse. The ratio of the normalized beat of the L1 component,  $B(L1, t)$ , to that of the L2 component,  $B(L2, t)$ , and that for the L3 and L4 components are, respectively, given by

$$R_{12} = \frac{B(L1, t)}{B(L2, t)} = \frac{\alpha^2 + \kappa^2}{\kappa^2 \alpha^2 + 1} \quad (5a)$$

and

$$R_{34} = \frac{B(L3, t)}{B(L4, t)} = \frac{\beta^2 + \kappa^2}{\kappa^2 \beta^2 + 1} , \quad (5b)$$

where  $\kappa = \frac{\Gamma}{\sqrt{\Delta^2 + \Gamma^2}}$ ,  $\alpha = \left| \frac{\mu_{24}\mu_{41}}{\mu_{23}\mu_{31}} \right|$  and  $\beta = (\mu_{14}/\mu_{13})^2$ . Here  $\Delta = \frac{(\epsilon_4 - \epsilon_3)}{\hbar}$  and  $\mu_{mn}$  is the transition moment between the states  $m$  and  $n$ . The relaxation constant  $\Gamma$  is the average value of  $\Gamma_{af} - \Gamma_{aa} + \Gamma_S$ , where  $\Gamma_{af}$  is the dephasing constant between the resonant state  $a$  and the final state  $f$ ,  $\Gamma_{aa}$  is the decay constant of the resonant state  $a$ , and  $\Gamma_S$  represents the spectral resolution of the detector. The subscripts to  $R$  refer to the transition states in a way that there are four states 1 through 4 to the whole structure. In the biased asymmetric DQW, the first two states 1 and 2 are almost localized in the NW and the WW, respectively and have been called the ground states of the NW and WW, while the other two excited states are expressed as

$$|3\rangle = \cos \theta |N_2\rangle + \sin \theta |W_2\rangle \quad (6a)$$

and

$$|4\rangle = \sin \theta |N_2\rangle - \cos \theta |W_2\rangle, \quad (6b)$$

where the angle  $\theta$  is determined by the magnitude of the tunneling interaction between the zeroth-order states  $|N_2\rangle$  and  $|W_2\rangle$ .

From these expressions, we can obtain  $\alpha = 1$  which gives  $R_{12} = 1$ . Since the value of  $\alpha$  is not dependent on the value of the bias voltage, the normalized beat of the two out-of-phase components always show the same beat modulation depths (ideally, 100% modulation<sup>3</sup>). Of course, the slight deviation seen in Fig. 4 is attributed to the breakdown of the approximation that the first two states are localized in either wells. On the other hand, the parameter  $\beta$  is given by  $\beta = \tan^2 \theta$ , so that the in-phase beats do not have the same modulation depths except in the resonant case of the bias voltage. It should be noted that since the ratio  $R_{34}$  is expressed in terms of the parameter  $\beta$  and the experimentally-determinable parameter  $\kappa$ , by measuring the ratio  $R_{34}$ , it should be possible to estimate the magnitude of the interaction between the two zeroth-order excited states  $|N_2\rangle$  and  $|W_2\rangle$ , i.e., the magnitude of the tunneling interaction.

The above analysis is based on the assumption that both the initial and final states are well-localized states in either well. This assumption is not valid in the DQW with the thin middle barrier; however, a similar analysis is possible even in such cases, but under restricted conditions. If the value of the bias voltage satisfies the resonance condition, the excited states  $|3\rangle$  and  $|4\rangle$  are expressed as completely symmetric and antisymmetric combinations of the single QW states  $|N_2\rangle$  and  $|W_2\rangle$ . These special forms of the resonant states give the following simple expressions for  $\alpha$  and  $\beta$ :

$$\alpha = \frac{\gamma \tan \phi + 1}{\gamma \tan \phi - 1} \frac{\gamma - \tan \phi}{\gamma + \tan \phi} \quad (7a)$$

and

$$\beta = \left\{ \frac{\gamma - \tan \phi}{\gamma + \tan \phi} \right\}^2, \quad (7b)$$

where  $\gamma$  is a constant, and the angle  $\phi$  determines the magnitude of the tunneling interaction between the zeroth-order states  $|N_1\rangle$  and  $|W_1\rangle$ ,

$$|1\rangle = \cos \phi |N_1\rangle + \sin \phi |W_1\rangle \quad (8a)$$

and

$$|2\rangle = \sin \phi |N_1\rangle - \cos \phi |W_1\rangle. \quad (8b)$$

Finally, we would also like to note another possible excitation and detection scheme. According to the DQW system employed by Leo et al<sup>2</sup>, the following scheme is also possible:

$$\begin{array}{ccc} LH \xrightarrow[\text{excitation}]{\text{pulsed}} & WW \leftarrow \text{tunneling} \rightarrow & NW \\ \downarrow & & \downarrow \\ LH & & HH \end{array},$$

where LH and HH denote the light-hole and heavy-hole states, respectively.

In conclusion, we have numerically calculated the luminescence intensity from a biased asymmetric DQW. In the case where the initial and final states are localized in either well, the out-of-phase beats always have the same normalized beat modulation depths, independent of the magnitude of the tunneling interaction within the resonant states, while the in-phase beats do not have the same modulation depths except in the resonant bias-voltage case. From the ratio of these normalized beat modulations of the in-phase beats, it could be possible to estimate the magnitude of the tunneling interaction. In the case where the initial and final states are delocalized in both wells, we have proposed a similar scheme for determining the magnitude of the tunneling interaction within these two lowest states.

We appreciate helpful discussion with Dr. Mark I. Stockman, and one of us (YO) would like to thank Professor T. Abe and Dr. H. Kono for helpful suggestions. This work was supported by the Office of Naval Research and the National Science Foundation under Grant CHE-9196214.



## References

- † Permanent Address: Department of Chemistry, College of General Education, Tohoku University, Kawauchi, Aoba-ku, Sendai 980, Japan
1. G. Bastard, *Wave Mechanics Applied to Semiconductor Heterostructures* (Les Editions de Physique, Les Ulis, France, 1988).
  2. K. Leo, J. Shah, E. O. Gobel, T. C. Damen, S. Schmitt-Rink, W. Schaefer and K. Kohler, *Phys. Rev. Lett.* **66**, 201 (1991).
  3. P. M. Felker and A. H. Zewail, *Phys. Rev. Lett.* **53**, 201 (1991).
  4. S. Luryi, *Solid State Commun.* **65**, 787 (1988).
  5. M. I. Stockman, L. N. Pandey and T. F. George, *Phys. Rev. Lett.* **65**, 3433 (1990).
  6. M. I. Stockman, L. S. Muratov, L. N. Pandey T. F. George, *Phys. Lett. A*, in press (1992).
  7. M. I. Stockman, L. S. Muratov, L. N. Pandey T. F. George, *Phys. Rev. B*, in press (1992).
  8. G. S. Agarwal, *Phys. Rev. Lett.* **37**, 1383 (1976); J. H. Eberly, *ibid.* **37**, 1387 (1976).
  9. The barrier height and effective mass depend on  $y$ , the fraction of *Al* in the layer of *AlGaAs* forming the barrier. The number of monolayers of *AlGaAs* and *GaAs* define the widths of the barrier and well, respectively. The barrier height is calculated by the formula  $V_i(\text{eV}) = 0.65(1.155y + 0.37y^2)$  and effective mass by  $\frac{m^*}{m_0} = 0.067 + 0.088y$ , where  $m_0$  is the mass of the bare electron. These formulae are given in detail in a phenomenological study by H. J. Lee, L. Y. Juravel, J. C. Woolley and A. J. SpringThorpe, *Phys. Rev. B* **21**, 659 (1980).
  10. L. N. Pandey and T. F. George, *J. Appl. Phys.* **69**, 2711 (1991).
  11. L. N. Pandey and T. F. George, *Superlattices and Microstructures* **10**, 5 (1991).
  12. The values of the relaxation parameters are chosen so as to have the same magnitude as those observed in Reference 2.
  13. L. F. Mollenauer, R. M. Stolen, J. P. Gordon and W. J. Tomlinson, *Opt. Lett.* **8**, 289 (1983).
  14. (a) S. Shapiro, R. Cavanagh and J. Stephenson, *Opt. Lett.* **6**, 470 (1981); (b) M. A. Kahlow, W. Jarzeba, T. P. DuBruil and P. F. Barbara, *Rev. Sci. Instrum.* **59**, 1098 (1988).
  15. The Markoff approximation usually overestimates the spectral-wing intensity of the luminescence, so that in the off-resonance bias voltage case, the quantum beat modulation of the L4 component could be enlarged by the tail part of the L3 component.

### Figure Captions

Fig. 1. Illustration of the biased asymmetric DQW along with the energies for four states  $|N_1\rangle$ ,  $|N_2\rangle$ ,  $|W_1\rangle$  and  $|W_2\rangle$  at the resonant bias voltage of 6.36 kV/cm.

Fig. 2. Stationary luminescence spectra in the resonance case of the bias voltage (a) and in the off-resonance case (b). The central energy of the incident light is tuned to be the average of the energies of the resonant states  $|N_2\rangle$  and  $|W_2\rangle$ . The spectral widths of the incident and scattered lights are assumed to be  $\Gamma_I = \Gamma_S = 0.05$  meV. For the relaxation parameters, we employ the following values (in the unit of meV)<sup>12</sup>:  $\gamma_1 = 0.0$ ,  $\gamma_2 = 1.0 \times 10^{-3}$ ,  $\gamma_3 = \gamma_4 = 1.0 \times 10^{-2}$ ,  $\gamma_{13}^{(pd)} = \gamma_{14}^{(pd)} = \gamma_{23}^{(pd)} = \gamma_{24}^{(pd)} = 0.8$  and  $\gamma_{34}^{(pd)} = 0.3$ .

Fig. 3. Luminescence decay curves in the resonance case (a) and the off-resonance case (b). The solid and dashed lines represent the decay curves associated with the luminescence components L3 and L1, respectively. The dotted line in (a) shows the pulse envelope function, which has about a 330-fs FWHM and corresponding coherent spectral width, 2.0 meV. The spectral resolution of the detector is also set to be 2.0 meV. As for the relaxation parameters, we employ the same values as those in Fig. 2.

Fig. 4. Left-hand side: Normalized beat modulations of the out-of-phase beats in the resonance case (a) and the off-resonance case (b). The solid and dashed lines, respectively, denote the normalized quantum beats associated with the L1 and L2 luminescence components. All the parameters are set in value to be the same as those in Fig. 3.

Right-hand side: Normalized beat modulations of the in-phase beats in the resonance case (a) and the off-resonance case (b). The solid and dashed lines, respectively, denote the normalized quantum beats associated with the L3 and L4 luminescence components. All the parameter values are set to be the same as those in Fig. 3.

Fig. 1  
Ohtsuki, Pandey & George

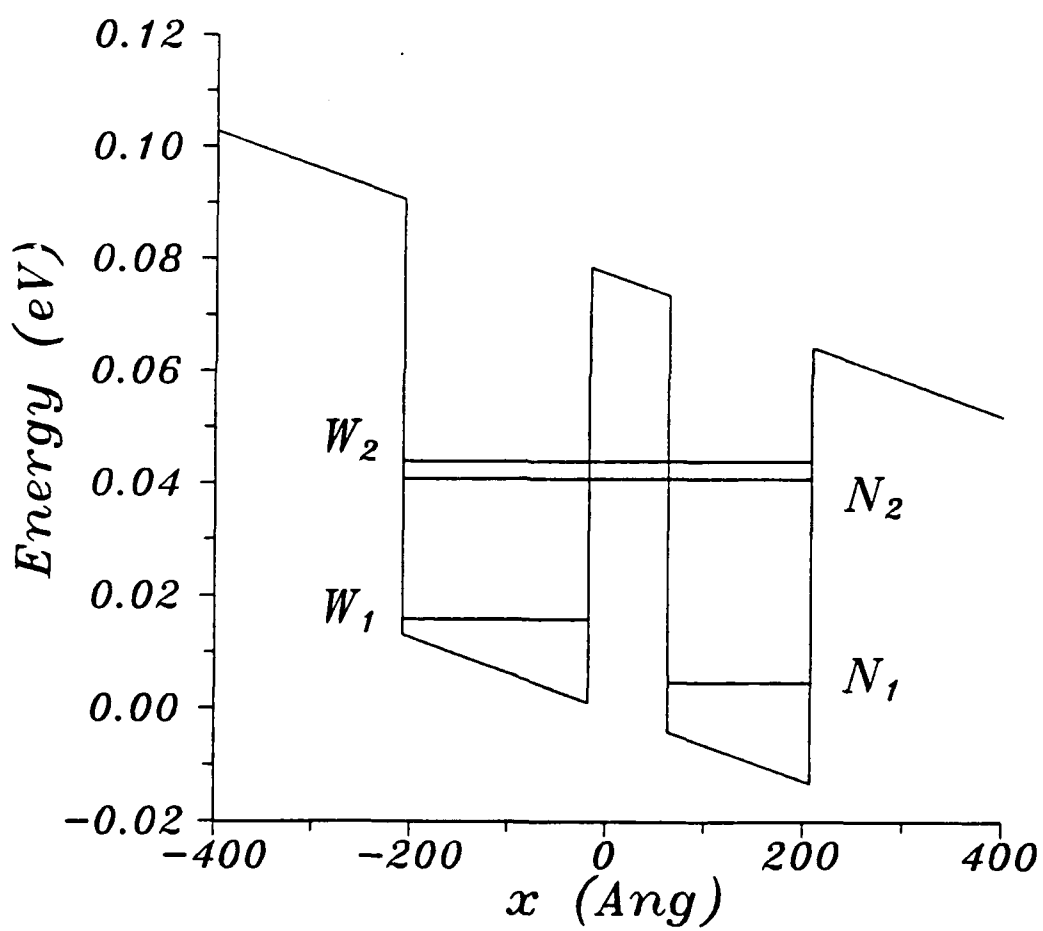


Fig. 2  
Ohtsuki, Pandey & George

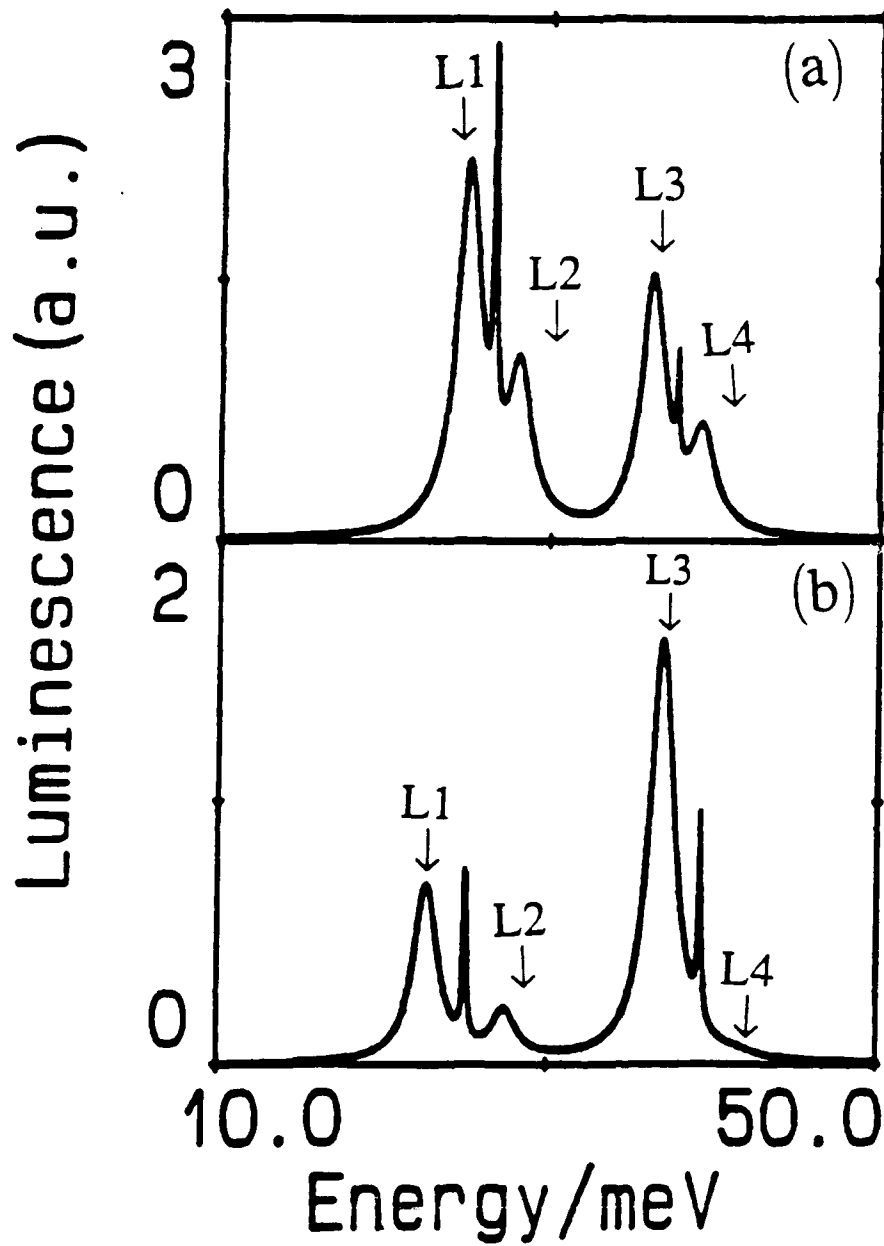


Fig. 3  
Ohtsuki, Pandey & Georj.

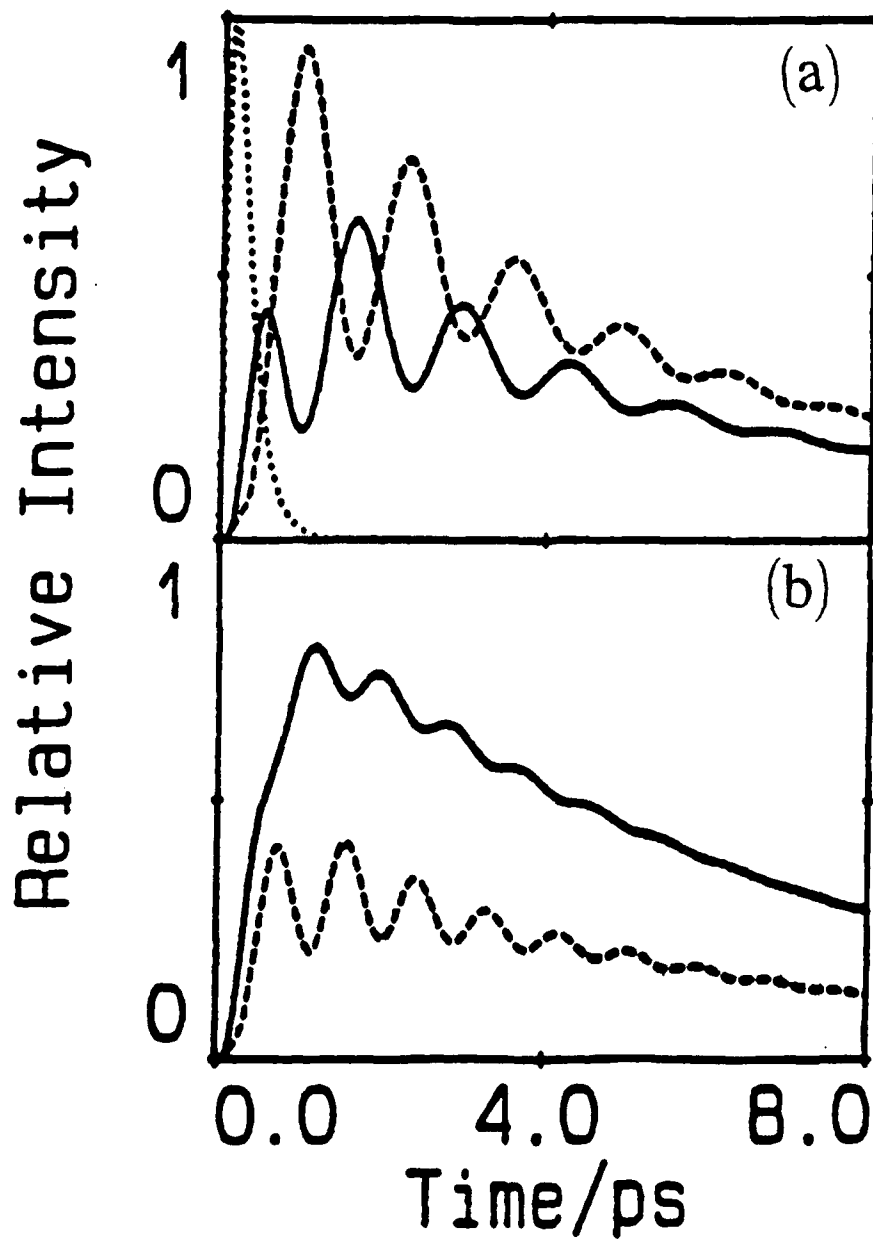


Fig.4  
Ohtsuki, Pandey & George

